ELECTRONIC SUPPORTING INFORMATION (ESI)

Understanding C-H activation in light alkanes over Cu-MOR zeolites by coupling advanced spectroscopy and temperature-programmed reduction experiments

Karoline Kvande,[a] Beatrice Garetto,[b] Gabriele Deplano,[b] Matteo Signorile,[b] Bjørn Gading Solemsli,[a] Sebastian Prodinger,[a] Unni Olsbye,[a] Pablo Beato,[c] Silvia Bordiga,[b] Stian Svelle,[a,*] and Elisa Borfecchia[b,*]

[a] Centre for Materials Science and Nanotechnology (SMN), Department of Chemistry, University of Oslo, 1033 Blindern, 0315, Oslo, Norway
[b] Department of Chemistry, NIS Center and INSTM Reference Center, University of Turin, via P. Giuria 7, 10125 Turin, Italy
[c] Topsoe A/S, Haldor Topsøes Allé 1, DK-2800 Kgs. Lyngby, Denmark

* Corresponding authors:
elisa.borfecchia@unito.it (E.B.)
stian.svelle@kjemi.uio.no (S.S.)

Table of Contents

1 Additional results and comments on Cu-MOR XANES spectra

Figure S1a reports representative Cu K-edge XAS spectra (in the typical XANES range from 8970 to 9020 eV) related to the main pretreatment steps of the experiment, compared between the two studied Cu-MOR samples:

- "Ramp500" stands for the thermal treatment of Cu-MOR samples from RT up to 500°C in O_2;
- "Cool200" stands for the decreasing in temperature from 500°C to 200°C, always under O_2 gas flow;
- "Cool120" stands for the decreasing in temperature between 200°C and 120°C under He gas flow.

XANES data collected along the static step at 500 °C in O_2 are not shown here for brevity. At this stage, spectral modifications are hardly appreciable, consistent with the stable MCR-ALS concentration profiles observed for the relevant Cu-species in this part of the *in situ* experiments (see **Figure 2b**, main text).

During the heating ramp in O_2, the peak related to Cu^I 1s→4p manifests itself at intermediate temperatures, but then progressively decreases, in parallel with the WL intensity. This behavior reasonably points to a transient auto-reduction to Cu^I involving a relatively small fraction of the Cu ions, which is however completely lost at the end of the process, giving way to a virtually pure Cu^{II} state.[1] Since this transient auto-reduction is explained previously, and involves different Cu^{II} and Cu^I species, we decided to exclude this region from the MCR-ALS analysis to have the most optimal starting point for the analysis tool. In the "Cool200" and "Cool120" experimental steps, no further changes in the oxidation state of the Cu species are found. Yet, a slight increase in the WL intensity observed when the temperature decreases, suggests minor changes in the local Cu coordination environment.

Figure S1b complements the Cu K-edge XANES results reported in **Figure 1** (main text) during TPR, showing a magnification of the XANES energy region related to 1s → 3d transition in Cu^{II} ions. It is evident that the Cu^{II} fingerprint peak at ca. 8977 eV is present in both samples at the beginning of the TPR step, and it is progressively eroded as temperature increases. In the final state at 550 °C, the pre-edge peak is no longer detectable, indicating a full reduction to Cu^I within the conventional XAS detection limit of ca. 5% total Cu.

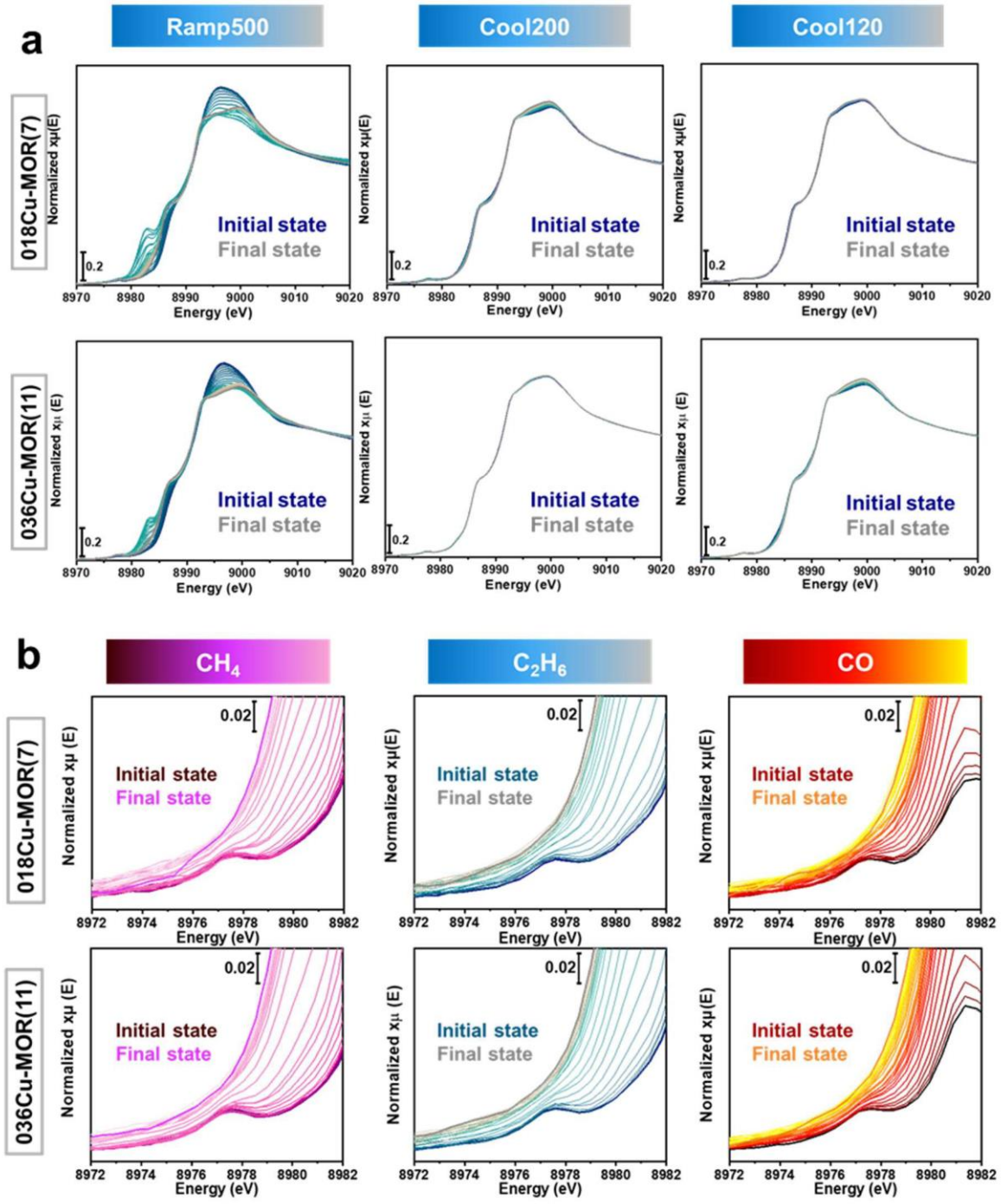

Figure S1. (a) XANES spectra for both 018Cu-MOR(7) and 036Cu-MOR(11) samples collected during the main pretreatment steps, before C_2H_6-TPR experiments. These data are selected as representative of all the experiments, where the same behavior is always observed along these steps. (b) Magnification of the XANES energy region related to 1s → 3d transition in Cu^{II} ions. Herein, spectra for both 018Cu-MOR(7) and 036Cu-MOR(11) samples collected during the TPR step are reported.

2 MCR-ALS analysis on Cu-MOR *in situ* XAS spectra

As reported in the main text, Multivariate Curve Resolution - Alternating Least Squares (MCR-ALS) is applied to the *in situ* XAS dataset. This advanced data analysis method allows the decomposition of an experimental series of spectra expressed in the form of a data matrix, into two main matrices: consisting of concentration profiles and the corresponding spectra of each chemical species present in the mixture.[2] Consequently, distinct chemical species (referred to as "pure") present different contributions in the system depending on their amount inside the sample:

$$\mu(E) = \sum^{N} c_i s_i(E) + \varepsilon \qquad \text{(S1)}$$

where N is the number of "pure" spectral compounds in the composition, E is the energy vector, $s_i(E)$ the energy-dependent "pure" spectrum and c_i the fractional abundance of s_i.[3] Under this assumption, the decomposition of (1) can occur exploiting the MCR-ALS approach, in which an iterative minimization is implemented, including only contributions coming from the original data matrix. Therefore, no initial structural models or reference data are needed for this type of analysis. Yet, to retrieve a reasonable solution from (1), some rules have to be followed by the operator:

- Sufficiently high amount of XAS spectra, showing a sufficient spectral variance
- Homogeneity in sampling the entire reaction process

The reason for this choice stands in the possibility to increase the probability to avoid errors and underestimations of the dataset rank, obtaining a uniform distribution of the variations of the XAS spectral features during the entire measurement.[3]
Going more specifically into the method, the MCS-ALS decomposition can be seen in terms of matrices. Assuming that D is a matrix composed of a set of experimental spectra collected on a variable of species, its decomposition into pure component spectra S matrix and the corresponding concentration profile C matrix can be expressed by eqn. (S2):

$$D = C \cdot S^{T} \qquad \text{(S2)}$$

where S^{T} is the transpose of matrix S.[4]

The first step of the algorithm requires the determination of the number N of principal components (PCs) that characterize the entire dataset and, consequently, the evaluation of the magnitude of each singular component.[5] The criterion used in this study for the determination of the PCs firstly involved analysis of Scree Plots for each sub-dataset, obtained by joining the data for the two Cu-MOR samples with the same reducing agent, namely CH_4, C_2H_6, and CO.

As illustrated in **Figure S2**, in all cases, Scree Plots showed a stepped or very smooth variance decrease, thus identifying a reasonable range rather than a well-resolved number of PCs. Several preliminary MCR-ALS reconstructions were thus performed, with N varied in the 4-6 range, and results, as well as consistency with previous literature findings. The best outcome was obtained in correspondence of $N = 4$ PCs in the case of CH_4-TPR, or $N = 5$ PCs in the case of C_2H_6 and CO-TPR.

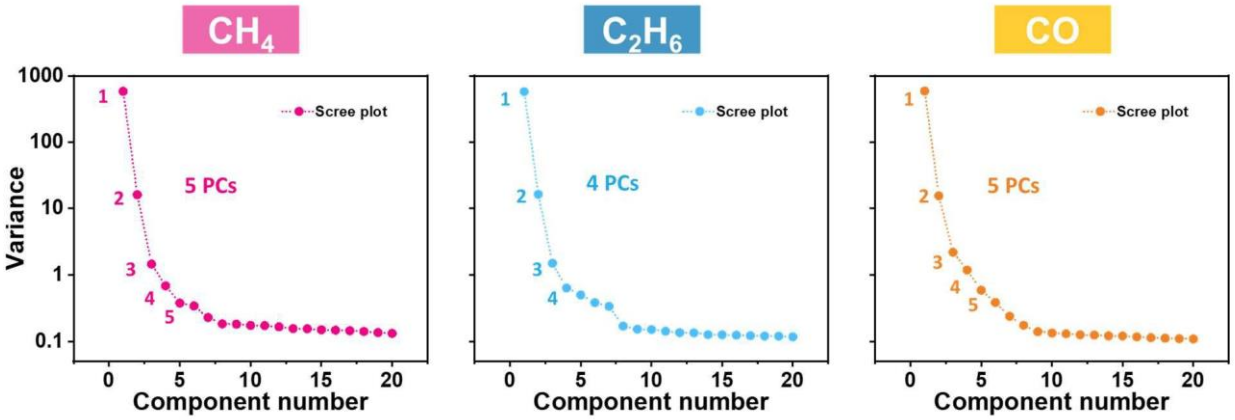

Figure S2. Scree Plots obtained for the three sub-datasets analyzed by MCR-ALS. Vertical dashed lines identify the number of PCs employed in the final MCR-ALS reconstructions.

The principal results that MCR-ALS returns are concentration profiles and spectra of pure components, and their generation depends on initial guesses, efficiently managed by specific methods, such as SIMPLISMA.[6] Afterwards, iterative optimization of the generated model is required until substantial (user-definable) differences between the model and two consecutive iterations are no longer found, meaning that convergence is achieved. In terms of accuracy, the MCR-ALS algorithm is affected by the *rotational ambiguity phenomenon*,[7] consisting of the possible existence of more than one model that can equally well describe the initial dataset. In these terms, a set of constraints needs to be introduced to reduce the ambiguity as much as possible, such as *non-negativity*, *unimodality*, and *closure*.[8]

Specific data treatment is required and depends on different assumptions linked to the analysis itself. First of all, the data used for MCR analysis are those obtained after the standard XAS data treatment using the Athena code,[9] i.e., the normalized and energy-aligned Cu K-edge XAS spectra. For the final purpose of the analysis, the initial pretreatment step, heating from RT to 500°C in O_2 (Figure S1, "ramp500"), is not considered. This choice was dictated by the fact that it was impossible to retrieve a spectroscopically and physicochemical meaningful MCR reconstruction for the whole dataset, including also this initial step. Most likely, this is due to the transient auto-reduction effect that is visible in the XANES spectra reported in Figure S1**,** implying the transient presence of a Cu^I species, always in very low concentration, which is not possible to faithfully reconstruct.

Under this assumption, the normalized μ(E) XAS spectra are then organized according to the reducing agent used during the TPR step, merging the datasets related to the two investigated samples, to prepare the file to be used as input for the MCR-ALS reconstruction. The latter is carried out using the MATLAB-based MCR-ALS Graphical User Interface (GUI)92.[8] As explained above, some constraints are needed; in this case, only soft constraints are applied: non-negativity for both concentration profiles and spectra, and closure to 1 for concentration profiles.

A series of quality indicators linked to the reconstruction is reported in **Table S1**-**Table S3**.

Table S1. Quality indicators of the MCR-ALS analysis (PCs = 5) of the *in situ* XAS dataset collected during CH_4-TPR

CH_4	
MCR-ALS Quality Indicator	**Value**
Std. Deviation of residual vs exp. Data	0,0019417
Fitting error (LOF) in (%) of PCA	0,057704
Fitting error (LOF) in (%) of exp.	0,21759
Iteration number to the convergence	52
Percentage of variance explained at the optimum	99,9995

Table S2. Quality indicators of the MCR-ALS analysis (PCs = 4) of the in situ XAS dataset collected during C_2H_6-TPR.

C_2H_6	
MCR-ALS Quality Indicator	**Value**
Std. Deviation of residual vs exp. Data	0,0016688
Fitting error (LOF) in (%) of PCA	0,04609
Fitting error (LOF) in (%) of exp.	0,18701
Iteration number to the convergence	56
Percentage of variance explained at the optimum	99,9997

Table S3. Quality indicators of the MCR-ALS analysis (PCs = 5) of the in situ XAS dataset collected during CO-TPR.

CO	
MCR-ALS Quality Indicator	**Value**
Std. Deviation of residual vs exp. Data	0,0015453
Fitting error (LOF) in (%) of PCA	0,050086
Fitting error (LOF) in (%) of exp.	0,17321
Iteration number to the convergence	60
Percentage of variance explained at the optimum	99,9997

3 Reproducibility of MCR-derived XANES spectra

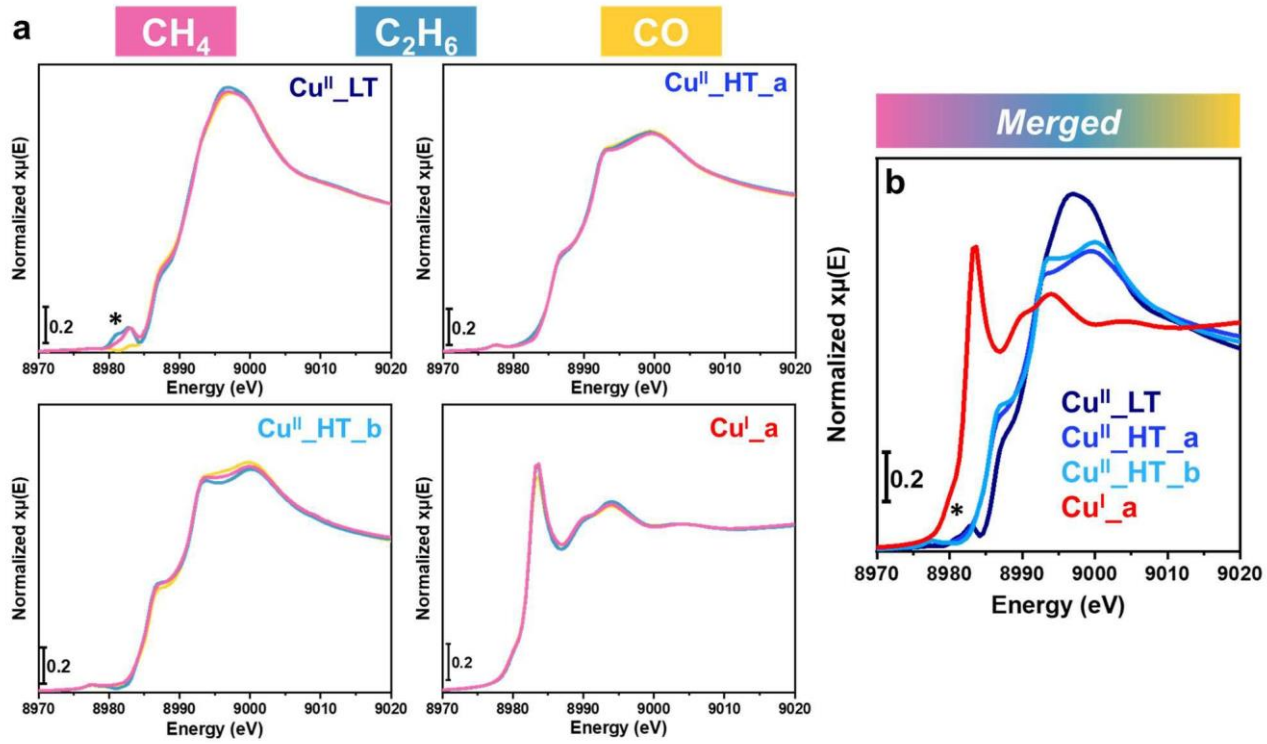

Figure S3. (a) Comparison between MCR-ALS XANES spectra obtained from the reconstruction of each sub-dataset (labeled according to the reducing agent used in the TPR step) for the four common pure Cu-species, found with very similar spectral signatures in all cases. (b) Resulting merged XANES curves for the four common Cu-species, reported and discussed in the main text. The * symbol in correspondence of individual and merged **Cu^{II} LT** spectra indicate an MCR reconstruction artifact.

Notwithstanding the use of different reducing agents, it can be noticed that four pure Cu-species are found with a very similar spectral signature in all the considered cases, meaning that Cu-speciation is largely conserved during the activation and, to a certain extent, the TPR step in our experiments. **Figure S3a** compares the individual MCR-ALS XANES spectra assigned to the same Cu pure species but coming from the three different sub-datasets. The excellent signal reproducibility observed for these Cu species in the XANES region comparing the three different reconstructions led us to merge their MCR-ALS XAS spectra, which are reported in **Figure S3b**, as well as in the main text.

4 Determination of reference temperatures for MCR-derived pure Cu-species

Table S4. Reference temperature values obtained for each Cu pure species, together with the average values.

Reducing agent	Sample	Temperature (°C)					
		Cu^{II}_LT	Cu^{II}_HT_a	Cu^{II}_HT_b	Cu^{I}_a	Cu^{I}_b	Cu^{I}_c
CH_4	018Cu-MOR(7)	283	396	343	436	-	-
	036Cu-MOR(11)	255	380	329	430	-	-
C_2H_6	018Cu-MOR(7)	281	378	353	451	414	-
	036Cu-MOR(11)	275	376	323	461	477	-
CO	018Cu-MOR(7)	233	392	355	480	-	318
	036Cu-MOR(11)	197	390	254	493	-	339
Average		254±33	385±8	326±37	458±24	446±44	329±15

Once MCR-ALS is performed on the experimental datasets, reference average temperature values $T_{i,ref}$ are evaluated for each i-th pure Cu species, allowing a better interpretation of the experimental results (**Table S4**).

Qualitatively speaking, $T_{i,ref}$ values indicate the temperature at which the PCs/pure Cu-species are most abundant, obtained applying the following eqn. (S3):

$$T_{i,ref} = \frac{\sum_j T_j \cdot c_{ij}}{\sum_j c_{ij}} \qquad \text{(S3)}$$

Here, at the numerator is reported the sum over all the experimental scans (index j) of the temperature T_j for the specific scan, weighted by the corresponding MCR-derived concentration c_{ij} for the i-th pure Cu species; at the denominator is reported the sum over all the scans of the c_{ij} values for the i-th pure Cu species. This procedure is repeated for each of the six pure species globally identified. The individual $T_{i,ref}$ values obtained for the two Cu-MOR samples, and, when possible, for the MCR-ALS reconstructions of different datasets, are further averaged and reported with their standard deviation in the bottom row of **Table S4**.

5 Extraction and reproducibility of MCR-derived EXAFS spectra

The data analysis reported in this supporting section follows the same procedure as applied to the XANES spectra. From the MCR-derived norm. μ(E) spectra presented above, having performed the MCR reconstruction including the whole, extended energy range, the EXAFS spectra were extracted according to the conventional procedures, as implemented into the Athena program. The obtained results, in both k (χ(k)) and R (χ(R)) domains, are visualized and commented on herein.

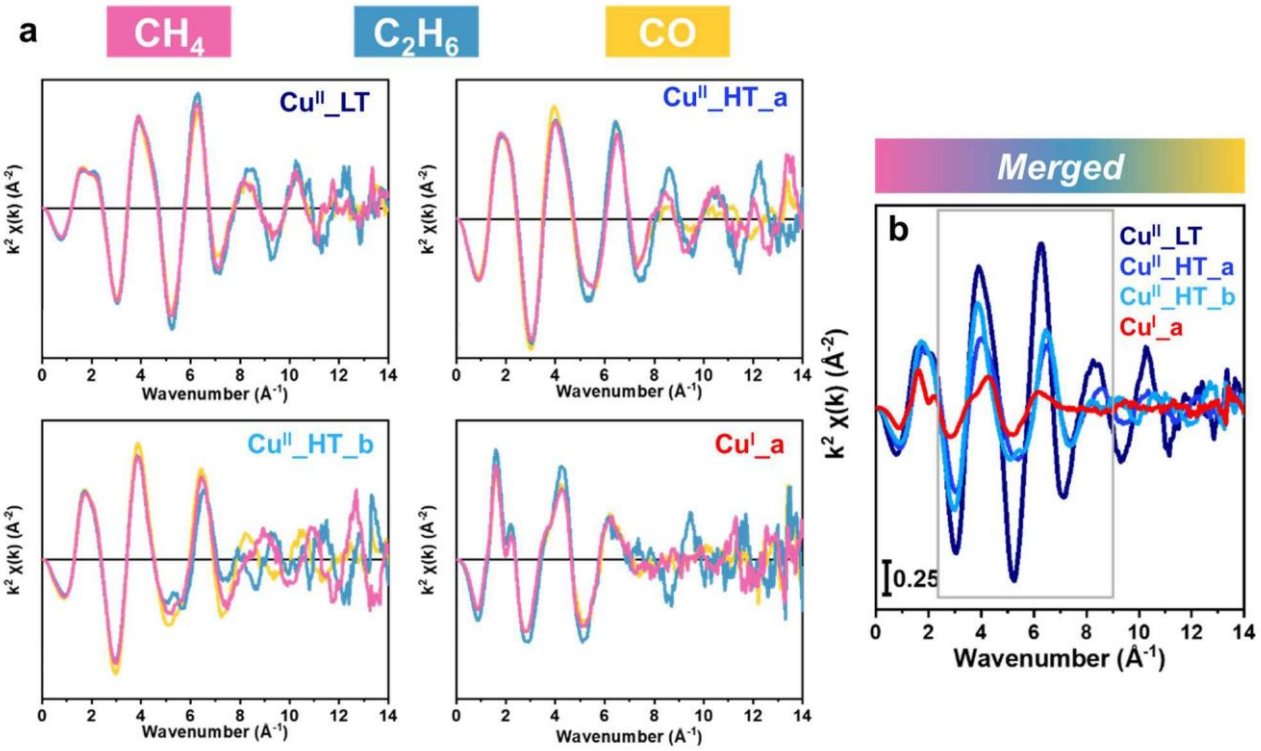

Figure S4. (a) Comparison between MCR-ALS $k^2\chi(k)$ EXAFS spectra obtained from the reconstruction of each sub-dataset (labeled according to the reducing agent used in the TPR step) for the four common pure Cu-species, found with very similar spectral signatures in all cases. (b) Resulting merged $k^2\chi(k)$ curves for the four common Cu-species, reported and discussed in the main text. The grey box in part (b) highlights the k-range chosen for conventional Fourier Transform (FT)-EXAFS analysis and subsequent Wavelet Transform (WT) analysis.

As done for the XANES region, **Figure S4a** reports the k-space $k^2\chi(k)$ EXAFS spectra of the pure Cu-species, common to the three sub-datasets corresponding to different reducing agents. Merging the three individual MCR-ALS derived EXAFS spectra appears, also in this case, a reasonable choice, since they have similar features according to the oscillation shape and frequency, at least at the beginning of the k-range.

Clearly, in the EXAFS region, we deal with a much weaker effective signal compared to the one in the XANES part, which mainly drives the MCR-ALS reconstruction. Thus, care must be taken in properly selecting the k-space range for further analysis by conventional Fourier Transform (FT) and Wavelet Transform (WT). By comparing the individual MCR-ALS derived EXAFS spectra, as well as the merged $k^2\chi(k)$ curves, we identified the 2.5-9.0 $Å^{-1}$ range (grey box in **Figure S4b**) as the safest balance between signal reproducibility and satisfactory S/N level.

Finally, we computed and compared the FT-EXAFS spectra obtained by transforming all the individual $k^2\chi(k)$ curves reported in **Figure S4a** in the selected 2.5-9.0 $Å^{-1}$ range. The results are

systematically reported in **Figure S5a**, using the same color/labeling scheme for pure Cu-species and sub-datasets.

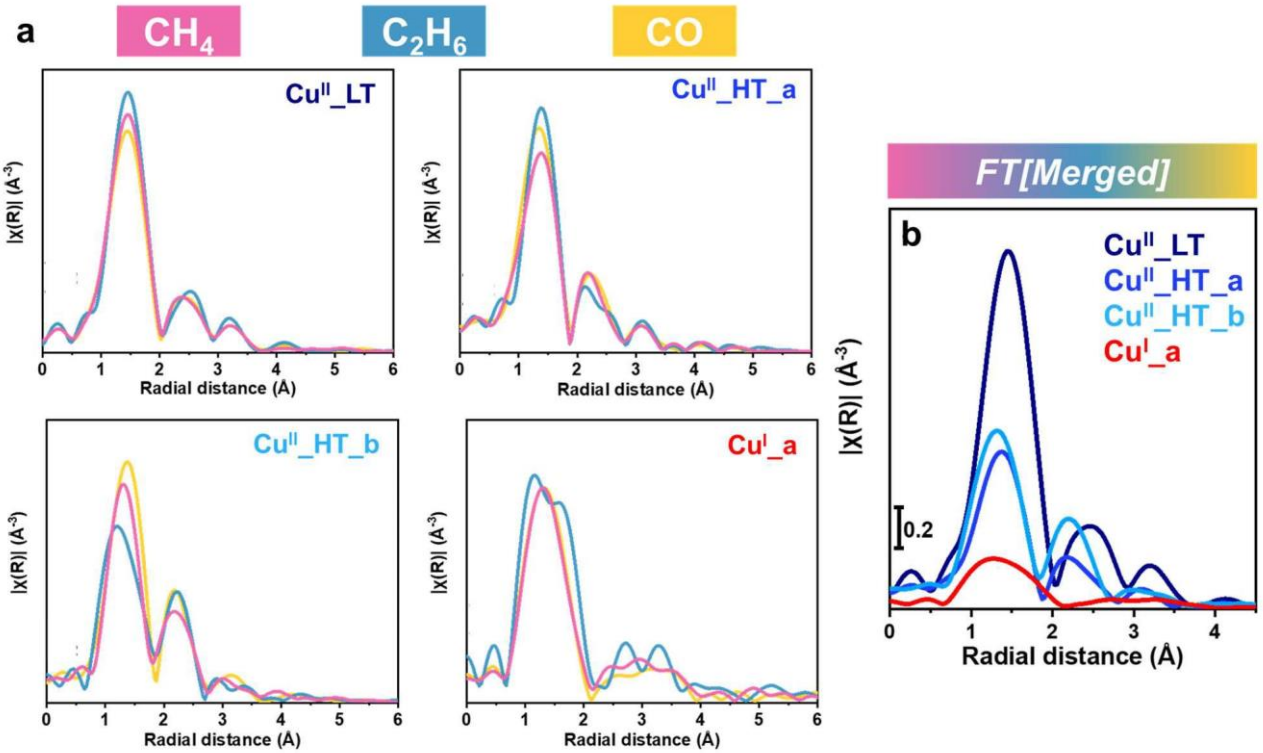

Figure S5. (a) Comparison between individual FT-EXAFS spectra for common Cu-species (labeled according to the reducing agent used in the TPR step) obtained transforming in the 2.5-9.0 Å^{-1} range the individual $k^2\chi(k)$ MCR-ALS EXAFS spectra in **Figure S4a**; (b) FT-EXAFS spectra for the four common Cu-species obtained transforming the merged $k^2\chi(k)$ curves in **Figure S4b** in the 2.5-9.0 Å^{-1} range, reported and discussed in the main text.

Spectroscopical fluctuations among the individual curves are visible, to a different extent depending on the Cu-species, as well as on their characteristic T_{red}. Yet, in all cases, the main EXAFS features - number, approximate position, intensity ratio of main peaks - are largely conserved, which justified further analysis on FT-EXAFS spectra obtained from the merged $k^2\chi(k)$ curves, reported in **Figure S5b**. In the **Cu^{I}_a** case, the individual scans show a poorer signal quality, and FT ripples are more evident. This is not surprising, since this Cu^{I} species shows the highest T_{red} throughout the series (see **Table S4**). In this case, the merging operation is particularly useful, leading to a substantial improvement in the FT-EXAFS signal quality for **Cu^{I}_a**, see the red curve in **Figure S5b**. Unfortunately, the same approach could not be applied to the MCR-ALS EXAFS spectra obtained for the two PCs/Cu-species solely present in one of the three sub-datasets, namely **Cu^{I}_b** and **Cu^{I}_c**. With this respect, the more challenging conditions realize for **Cu^{I}_b**, which is also associated to a T_{red} as high as 458 °C. Indeed, as discussed in the main text, for this Cu-species the WT-EXAFS maps show spurious signals from 8.0 Å^{-1} upward.

6 MS results obtained during *in situ* UV-vis spectroscopy

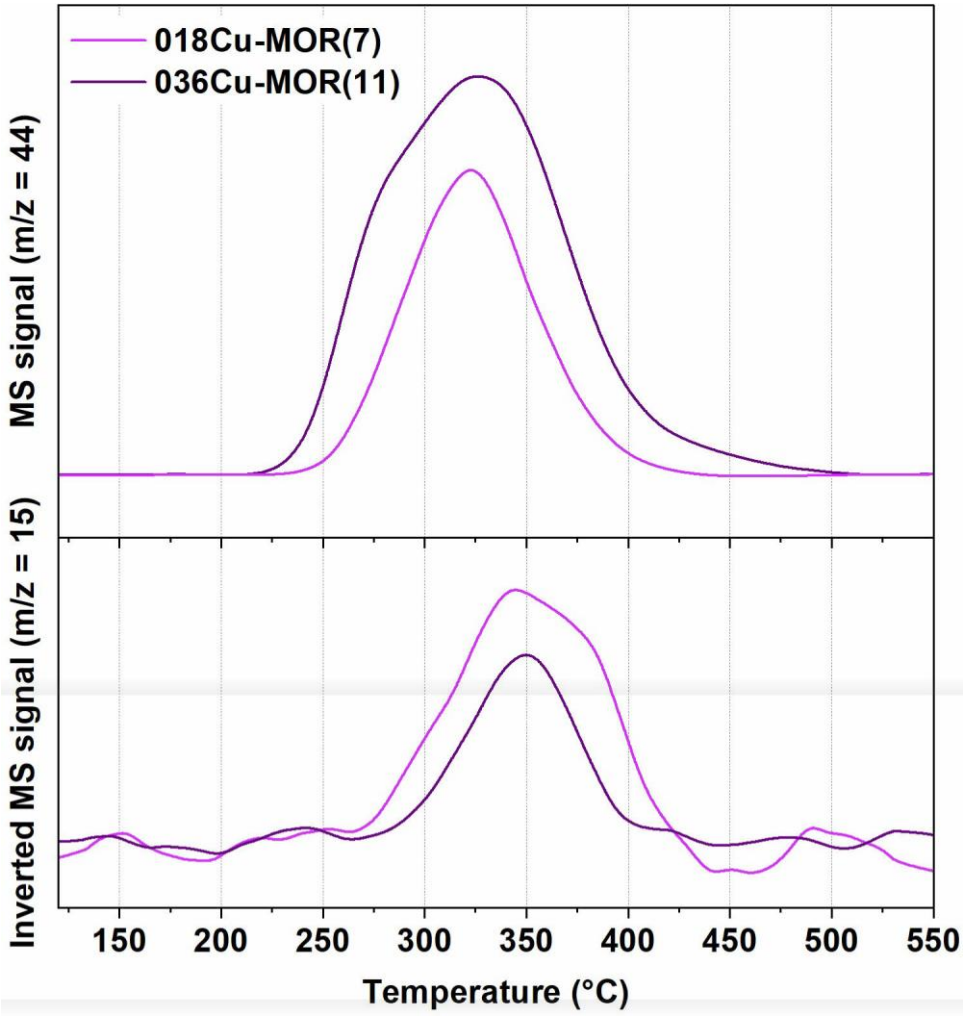

Figure S6. Comparison of the CO_2 formation (top panel) and CH_4 consumption (bottom panel) during the TPR protocol performed together with UV-vis measurements. The MS trace used for CO_2 is m/z = 44, while m/z = 15 is used for CH_4. The MS traces have been normalized to the sample weight and Cu content.

7 *In situ* FT-IR spectroscopy of CO-TPD experiment

The CO- temperature-programmed desorption (TPD) experiment was conducted on a Bruker Vertex 80 instrument equipped with a Mercury-Cadmium-Telluride (MCT) detector cooled with liquid nitrogen. The material was pressed into a thin, self-supporting wafer (10 mg) and placed inside an AABSPEC cell with low-free volume (model #CXX), where both temperature and gas flow can be controlled. The sample was heated to 500 °C (5 °C/min) in a flow of O_2 (100 %), before being cooled down to 120 °C (10 °C/min), where He (100 %) was purged on the sample for 1 h. Then, the gas flow was switched to CO (10 %/rest. He) for 30 min, and then the flow was switched back again to He (20 min) before the ramp was initiated. The sample was then ramped up to 500 °C (10 °C/min). One spectrum was collected every 40 s.

Figure S7 shows the CO-TPD spectra of 018Cu-MOR(7). The first band is collected at 120 °C after the sample had been flushed for 20 min in He. The band at 2158 cm^{-1} is the feature of monocarbonyl species interacting with Cu^I in MOR zeolites.[10] No bands related to dicarbonyl species are observed. However, a small shoulder is observed at 2140 cm^{-1}. This we allocate to CO and H_2O being co-adsorbed on Cu^I due to some moisture entering the system upon cooling.[11]

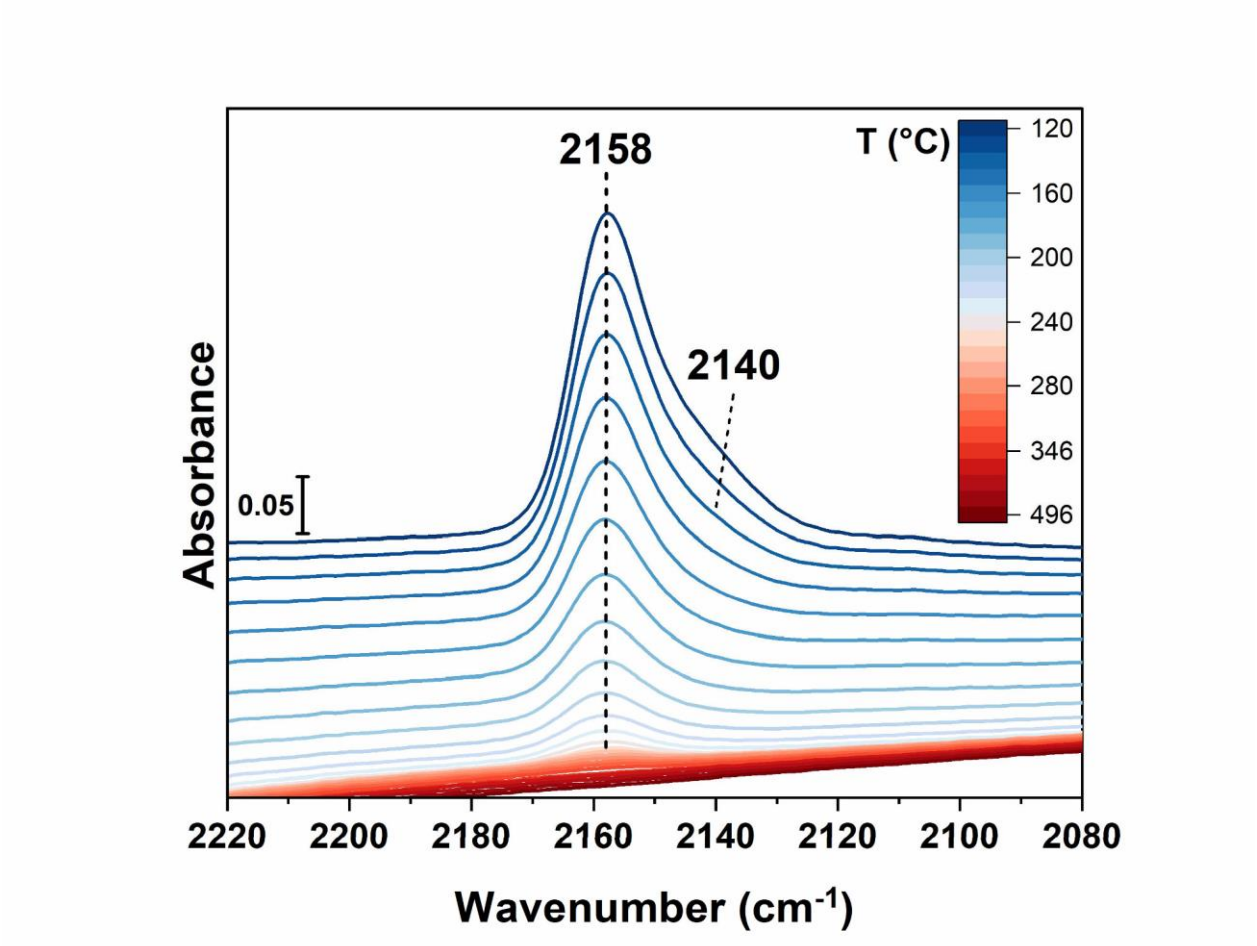

Figure S7. FT-IR spectra of the ν(CO) stretch region during CO-TPD on 018Cu-MOR(7).

References

1. V. L. Sushkevich and J. A. van Bokhoven, *Chem. Commun.*, 2018, **54**, 7447-7450.
2. W. H. Cassinelli, L. Martins, A. R. Passos, S. H. Pulcinelli, C. V. Santilli, A. Rochet and V. Briois, *Catal. Today*, 2014, **229**, 114-122.
3. A. Martini and E. Borfecchia, *Crystals*, 2020, **10**.
4. A. Martini, E. Alladio and E. Borfecchia, *Top. Catal.*, 2018, **61**, 1396-1407.
5. E. R. Malinowski and D. G. Howery, *Factor analysis in chemistry*, Wiley New York, 1980.
6. W. Windig and J. Guilment, *Anal Chem*, 1991, **63**, 1425-1432.
7. A. de Juan and R. Tauler, *Analytica Chimica Acta*, 2021, **1145**, 59-78.
8. J. Jaumot, R. Gargallo, A. de Juan and R. Tauler, *Chemometrics and Intelligent Laboratory Systems*, 2005, **76**, 101-110.
9. B. Ravel and M. Newville, *J. Synchrotron Radiat.*, 2005, **12**, 537-541.
10. S. Bordiga, C. Lamberti, F. Bonino, A. Travert and F. Thibault-Starzyk, *Chem. Soc. Rev.*, 2015, **44**, 7262-7341.
11. K. I. Hadjiivanov, M. M. Kantcheva and D. G. Klissurski, *Journal of the Chemical Society, Faraday Transactions*, 1996, **92**, 4595-4600.